Local Structure in Terms of Nearest Neighbor Approach in C_4mim^+-Based Ionic Liquids: MD simulations.

Bogdan A. Marekha[1,2*], Volodymyr A. Koverga[1,3], Erwan Chesneau[1], Oleg N. Kalugin[3], Toshiyuki Takamuku[4], Pál Jedlovszky[5,6] and Abdenacer Idrissi[1*]

[1]University of Lille, Science and Technology, LASIR (UMR CNRS A8516), Bât. C5, Cité Scientifique, 59655, Villeneuve d'Ascq Cedex, France

[2]UNICAEN, CERMN (Centre d'Etudes et de Recherche sur le Médicament de Normandie) - FR CNRS INC3M, boulevard Becquerel, 14032 Caen Cedex, France

[3]Department of Inorganic Chemistry, V.N. Karazin Kharkiv National University, Svobody sq., 4, Kharkiv, 61022, Ukraine

[4]Department of Chemistry and Applied Chemistry, Graduate School of Science and Engineering, Saga University, Honjo-machi, Saga 840-8502, Japan

[5]Department of Chemistry, Eszterházy Károly University, Leányka utca 6, H-3300 Eger, Hungary

[6]MTA-BME Research Group of Technical Analytical Chemistry, Szt. Gellért tér 4, H-1111 Budapest, Hungary

Corresponding authors' contact info:

bogdan.marekha@unicaen.fr

+33 (0)2 31 56 68 24
B.A.M.

nacer.idrissi@univ-lille1.fr

+33 (0)3 20 43 66 62
A.I.

Abstract

Description of the local microscopic structure in ionic liquids (Ils) is a prerequisite in obtaining a comprehensive understanding of the influence of the nature of ions on the properties of ILs. It is mainly determined by the spatial arrangement of the nearest neighboring ions. Therefore, the main interaction patterns in ILs such as cation-anion H-bond-like motifs, cation-cation alkyl tail aggregation and ring stacking were considered within the framework of the nearest neighbor approach with respect to each particular interaction site. We employed classical molecular dynamics (MD) simulations to study in detail the spatial, radial, and orientational relative distribution of ions in a set of imidazolium-based ILs, in which the 1-butyl-3-methylimidazolium (C_4mim^+) cation is coupled with the acetate (OAc^-), chloride (Cl^-), tetrafluoroborate (BF_4^-), hexafluorophosphate (PF_6^-), trifluoromethanesulfonate (TfO^-), and bis(trifluoromethanesulfonyl)amide ($TFSA^-$) anion. It was established that several structural properties are strongly anion-specific, while some can be treated as universally applicable to ILs regardless of the nature of anion. Namely, strongly basic anions, such as OAc^- and Cl^- prefer to be located in the imidazolium ring plane next to the $C\text{-}H^{2/4\text{-}5}$ sites. By contrast, the other four bulky and weakly coordinating anions tend to occupy positions above/below the plane. Similarly, the H-bond-like interactions involving the H^2 site are found to be particularly enhanced in comparison with the ones at $H^{4\text{-}5}$ in the case of asymmetric and/or more basic anions (C_4mimOAc, C_4mimCl, C_4mimTfO, and C_4mimTFSA), in accordance with recent spectroscopic and theoretical findings. Other IL-specific details related to the multiple H-bond-like binding and cation stacking issues are also discussed in the paper. The secondary H-bonding of anions with the alkyl hydrogen atoms of cations as well as the cation-cation alkyl chain aggregation turned out to be poorly sensitive to the nature of the anion.

1. Introduction

Room temperature organic molten salts, often referred to as ionic liquids (ILs) constitute a matter of a booming research interest due to a number of particular properties (negligible volatility, high solvating power towards both organics and inorganics, thermal and electrochemical stability etc.) rendering them very promising in such industrial applications as electrochemical energy storage devices, media for dissolution and processing of biopolymers, or reaction and separation media to name a few.[1-2] As the number of possible counterion combinations is essentially countless and the cost of ILs is still rather high, their systematic experimental investigations are somewhat limited. In this regard computational and theoretical methods of research, in particular, atomistic simulations utilizing classical and/or *ab initio* force fields, represent a valuable complement and sometimes even an alternative to otherwise unfeasible experiments with ILs and IL-based systems.[3-5]

Despite an unprecedentedly detailed description of various structural and dynamical properties that can be accessible from molecular simulations, analysis of the results of such simulations is very often based solely on the radial distribution functions (RDFs) between centers of mass.[6-10] Moreover, many seminal computational studies on ILs have been performed either on a single IL or on a rather narrow family of systems, *e.g.*, chlorides, for the sake of computational efficiency, while the results have been presented as universally applicable.[3, 11-12] However, such claims can turn out to be questionable.

Thus, in ILs bearing 1-alkyl-3-methlylimidazolium cation ($C_n mim^+$, see Figure 1 for molecular structure and atom labeling in C_4mim^+) it is generally accepted that C-H^2 is the main H-bond donating site of the cation[13-16] and H-bonding at the rear of the imidazolium ring, *i.e.*, at H^{4-5}, is often dropped out of discussion. However, as it has been recently highlighted by us for a set of neat C_4mim^+-based ILs and for mixtures with acetonitrile,[17-18] as well as for a similar set of ion pairs considered in simulations of neat ILs by Matthews *et al.*,[10] the relative strength of H-bonding at H^2 and H^{4-5} sites is remarkably anion-dependent.

Another prominent example concerns the potential energy surface describing the position of anion in the vicinity of C_nmim^+ cations. On the basis of model quantum-chemical calculations and molecular dynamics (MD) simulations of $C_n$mimCl Zahn *et al.* proposed a paradigm of energy landscape relating the mobility of anions with melting points decrease.[19] However, as we have shown later in this paper, the mentioned potential energy profile is strikingly different between ILs bearing Cl^- anion and multiatomic anions with delocalized charge distribution, such as BF_4^-.[18]

All these findings highlight the need for detailed and systematic studies of ILs by means of molecular simulations. Here the term 'detailed' refers to the atomic-level description of the local structure around particularly relevant interaction sites, whereas 'systematic' implies a thoughtful selection of systems to be studied so that the eventual conclusions could be of use for the subsequent design of novel better performing ILs.[1-3, 20] Despite the fact that even the crudest MD force-fields describe the bulk thermodynamic properties of ILs relatively well,[21] it is the description of the local microscopic structure that is of interest for deciphering some spectroscopic findings[17, 22-24] or rationalizing their performance in such applications as catalysis[25] or cellulose dissolution[26].

A great deal of systematic MD studies on imidazolium ILs has been devoted to the issue of the alkyl chain length in C_nmim^+ cations, as it has direct implications on the microscopic heterogeneity, *i.e.*, the segregation of non-polar alkyl and polar ionic domains.[3, 27-30] Regarding the use of molecular simulations in explaining various spectroscopic observations one has to keep in mind that the vast majority of such experimental information reports the local molecular environment around specific sites of IL cations, *e.g.*, ^{1}H NMR signals, CH vibrational bands, etc.[22-23, 31-34] The importance of studying the influence of the anions on the microscopic structure around a reference cation is evident in this context.

Several MD works have focused on the influence of anions on the microscopic structure and dynamics in ILs[10, 35-36], however, the extent of site-specific information extracted from the simulations is rather limited. Nonetheless, we highlight the works of Kirchner *et al.*[37-39] in which the systematic selection of anions has been combined with a detailed analysis of the microscopic structure. Namely, they have investigated such aspects as cation-anion H-bonding, relative counterion arrangement, and different modes of cation aggregation in systems such as C_2mimOAc/Cl/SCN,[37] C_4mimOAc/CF_3COO/TFSA/TfO/Br/I,[39] and their analogues with fluorinated cations, and C_2mimSCN/$N(CN)_2$/$B(CN)_4$.[38]

Here we present a systematic MD study on the local microscopic structure around cations in six imidazolium-based ILs containing 1-butyl-3-methylimidazolium C_4mim^+ cation coupled with the acetate OAc^-, chloride Cl^-, tetrafluoroborate BF_4^-, hexafluorophosphate PF_6^-, trifluoromethanesulfonate TfO^-, and bis(trifluoromethanesulfonyl)amide $TFSA^-$ [40] anions (see Figure 1 for molecular structures). The selected set of ILs is mainly of interest for such applications as biopolymer dissolution (C_4mimOAc and C_4mimCl)[26] and electrolytes for batteries and other energy related applications (C_4mimBF_4, C_4mimPF_6, C_4mimTfO, C_4mimTFSA).[41] We selected the C_4mim^+ cation as the associated ILs are liquids at room temperature (except C_4mimCl). Furthermore, both experimental and theoretical data are available in the literature on their microscopic structure, which provides the possibility of comparing them with our present results. By studying anions of different size, shape, symmetry, charge distribution and basicity we aim to reveal the influence of these anion properties on various fine aspects of the local structure in these systems, which is of great importance for fine-tuning the molecular design of novel ILs with better characteristics and for explaining numerous experimental findings.

Needless to say that any conclusions drawn on the local average preferential structure of ILs, should be treated with caution without proper handling of the corresponding dynamics.[38, 42] The latter constitutes the subject of our ongoing work, and will be presented in a subsequent publication. The rest of the paper is

organized as follows: MD simulation details are briefly presented in Section 2, the obtained results on the cation-anion relative arrangement, cation-anion H-bond-like interactions and cation-cation relative arrangement are discussed in Section 3, and, finally, Section 4 outlines the main conclusions of our work.

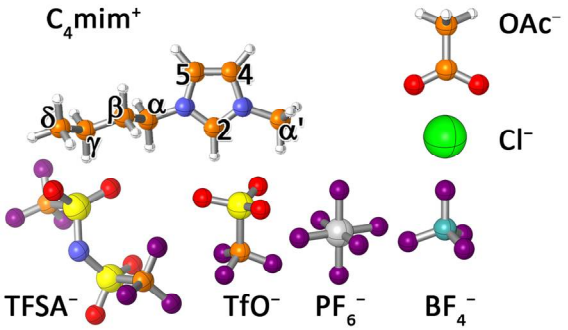

Figure 1. Molecular structures of C_4mim^+ cation and six anions constituting the studied ILs. Labeling of the CH sites in C_4mim^+ cation is also given. Color coding of the elements: white – H, orange – C, blue – N, red – O, green – Cl, cyan – B, purple – F, gray – P, yellow – S.

2. Computational details

All-atom MD simulations were performed with the DL_POLY_4 code (version 4.07).[43] Initial configurations of the systems were created with the Packmol software using the default closest contact tolerance of 2 Å.[44] The DL_FIELD tool was used in the preparation of the necessary force-field and configuration files.[45]

We employed the recent force-field model of Mondal and Balasubramanian[8-9] for all the ILs studied here. It is a scaled-charge non-polarizable model based on the popular force-field of Canongia Lopes and Pádua.[46-48] The model reproduces not only basic thermodynamic and structural properties but also a number of dynamical ones very well.[8-9, 49] Intramolecular degrees of freedom are represented by the corresponding bond stretching, valence angle bending, and dihedral rotation potentials. Several of these internal degrees of freedom were frozen in the simulations, namely, C-H bond stretches in C_4mim^+

cations and OAc^- anions, using the RATTLE algorithm,[50] while the BF_4^- and PF_6^- anions were treated as completely rigid bodies. The readers are referred to the original publications for the parameter values of the interaction potentials. We only note here that the original dihedral potential function is not implemented in the DL_POLY_4 code and it was thus refitted to an OPLS-type potential:

$$U(\varphi) = A_0 + 0.5\,(A_1\,(1 + \cos(\varphi - \varphi_0)) + A_2\,(1 - \cos(2(\varphi - \varphi_0))) + A_3\,(1+\cos(3(\varphi - \varphi_0)))) \quad (1)$$

The corresponding parameters are summarized in Table S1 in the Supporting Information.

For each system simulated, 864 ion pairs were randomly placed inside a cubic simulation box with three-dimensional periodic boundary conditions applied. Such a relatively large system size was selected by considering the results of Gabl *et al.*,[51] who claimed that sufficiently large system size (at least 512 ion pairs) and long simulation time are needed in order to properly capture both the structure and the dynamics of an ionic liquid. Moreover, they also emphasized that the number of particles is a more crucial factor in this respect than the length of the trajectory.[51] Electrostatic interactions were evaluated using the smoothed particle mesh Ewald technique with the real space cutoff of 15 Å and relative precision of 10^{-5}.[52] Non-bonded interactions were explicitly calculated within the spherical cutoff of 15 Å with the necessary long-range corrections to the system energy and pressure applied. Velocity Verlet integrator was used with the timestep of 2 fs. After initial energy minimization the systems were equilibrated for 1 ns on the isothermal-isobaric (*NpT*) ensemble at 300 K and 1 atm using Nosé-Hoover barostat[53] and thermostat[54] with relaxation constants of 2 ps and 0.1 ps, respectively. As C_4mimCl melts at a temperature higher than 300 K, this IL was simulated at 353 K in order to compare with the original publication of Mondal and Balasubramanian.[9] The simulated densities of all ILs studied here are in perfect numerical agreement with the originally reported values which, in turn, are quite close to the experimental data (see Table S2 in SI). The systems were further equilibrated for 5 ns on the canonical (*NVT*) ensemble using the Nosé-Hoover thermostat with the same relaxation constant. Production runs of

1 ns were performed afterwards, using the same parameters to produce 10000 independent sample configurations. All the analyses presented here were carried out using the TRAVIS code.[55]

3. Results and discussion

3.1. Cation-anion arrangement

We begin our analyses with a basic characterization of the relative arrangement of anions around a reference cation. Due to the different shape and symmetry of the anions considered in the present analysis, we describe their position via the corresponding atomic centers of coordinating group Y, *i.e.*, C^{COO} in OAc^-, Cl in Cl^-, B in BF_4^-, P in PF_6^-, S in TfO^- and $TFSA^-$. As most of the positive charge of the C_4mim^+ cation is localized at the imidazolium ring a typical approach is to consider the center of the ring (CoR) – Y radial distribution functions (RDFs).[39] However, these RDFs show little detail (see Figure S2) as they sample all the possible orientations of the vector connecting the reference and observed sites.

A common way to resolve the orientational component of these functions is to study the isosurfaces of the so-called spatial distribution functions (SDFs).[9-10, 35, 56-58] This type of representation, however, suffers from the somewhat ambiguous choice of the isovalue, and also from the lack of information on the distribution of the observed particle density inside the region enclosed by the isosurface. We overcome these difficulties by using the cross-sections of the spatial distribution functions CoR – Y with the observed particle density color-mapped on the slicing planes (see Figure S3). It is well known from numerous published conventional SDFs[9, 35, 56-58] that in imidazolium-based ILs anions prefer to occupy three main sites next to the ring CH sites with a higher intensities observed at the $C\text{-}H^2$ group and a minor one next to the $C^{\alpha'}H_3$ group. It is noteworthy that the latter is often overlooked because of too high SDF isovalue used. In this regard, one of the cutting planes shown in Figure S3 is the imidazolium ring plane while the other one is orthogonal to the first one and contains the $C\text{-}H^2$ line.

It is readily apparent from Figure S3 that all the aforementioned regions of localization of anions around a reference C_4mim^+ cation (*i.e.*, next to the imidazolium ring C-$H^{2/4-5}$ sites and in front of the $C^{\alpha'}H_3$ group) are observed in all the studied ILs. However, several IL-specific features are also apparent. Namely, the localization of anions becomes progressively more diffuse in the order of $OAc^- < Cl^- < BF_4^- \approx PF_6^- < TfO^- < TFSA^-$. In particular, around the C^2-H site the nature of the distribution of anions above/below and within the imidazolium ring plane is strongly anion dependent.

In order to study the latter aspect in more detail, we have decided to calculate the distribution of the first nearest neighboring anions with respect to cation's main sites of interest. Indeed, it is primarily the nearest neighbor that defines the local environment of a reference site. Thus, by analyzing different structural properties taking into account only the first nearest neighbors[59-61] one samples over a small yet significantly reasonable volume of space. In this regard, we described the position of the first nearest neighboring coordination group of anions with respect to one of the three ring hydrogen atoms $H^{2/4-5}$ of C_4mim^+ cation in terms of the distance H^i-Y and the angle φ_i between the imidazolium ring normal vector and the radius-vector H^i-Y (see Figure 2 for the scheme). Thus, a perfect in-plane arrangement of the observed anion next to the reference H^i site would correspond to the φ_i values around 90°, while positions above/below the reference site would contribute to the φ_i values close to 0 and 180°.

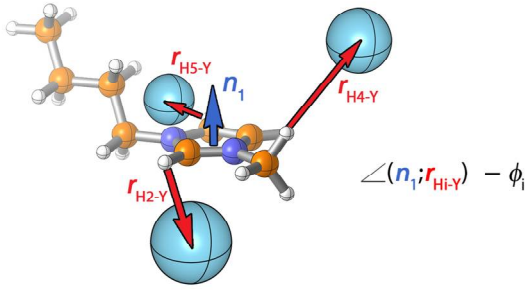

Figure 2. Schematic representation of the main parameters used for the description of the relative position of anion with respect to the imidazolium ring C-$H^{2/4-5}$ sites.

The results of the present analysis are shown in Figure 3A as combined distribution functions (CDFs) correlating the H^i-Y distances and the corresponding φ_i values for the first nearest neighboring anions with respect to $H^{2/4-5}$. By construction, these contour plots are very similar to the slicing plane in Figure S3 that contains the C-H^2 line. However, due to restriction to the first nearest neighbor with respect to each specific reference site these CDFs bring about more information.

A common point of all the studied ILs here is that both angular and radial distributions are more diffuse in the case of H^{4-5} than in the case of H^2. This means that the general position of the neighboring anion is better localized around the H^2 site, which obviously stems from its higher positive charge.[9, 12, 57] At the same time, there are still plenty of anion-specific information. For example, one can notice that OAc^- and Cl^- strongly prefer to occupy the in-plane positions around all the ring C-$H^{2/4-5}$ sites, although the CDF of Cl^- shows some tails towards above/below H^2 positions, as well. The four other anions, in contrast, show a distinct preference towards above/below H^2 arrangement. This effect is the most pronounced in C_4mimPF_6, then, to a similar extent, in C_4mimBF_4 and $C_4mimTfO$, while $C_4mimTFSA$ reveals the most diffuse anion distribution around the H^2 site. As for the distribution of the perfluorinated anions around the H^{4-5} atoms, some anion-specific details are also apparent. In C_4mimBF_4 and $C_4mimTfO$ the anions tend to be localized around the in-plane positions next to the H^{4-5} sites, while in $C_4mimTFSA$ the bulky anion is mainly found above and below these sites. In the latter case, one also has to notice that the distribution is even more diffuse than around H^2. Finally, PF_6^- occupies mainly in-plane position next to H^5, and slightly prefers the above/below H^4 arrangement.

Clearly, the above/below arrangement of the nearest neighboring anions around the imidazolium ring plays a non-negligible, if not the dominant (depending on the anion) role in determining the local microscopic structure around a reference C_4mim^+ cation. In an attempt to characterize such contributions that could have been overlooked in the analysis presented above, we studied the distribution of the nearest neighboring anions to the CoR that are, at the same time, *not* the first nearest neighbors of any of the

imidazolium ring C- $H^{2/4-5}$ sites, and hence have not been taken into account in the previous analysis. Figure 3B presents the results of this analysis in the form of contour plots of the density of projections of the anion position to the imidazolium ring plane. The percentages shown in the plots indicate the fraction of the nearest to the CoR anions that satisfy the second condition, *i.e.*, not being the nearest neighbors of any of $H^{2/4-5}$.

In accordance with what has been found above, there is a rather low probability of finding OAc^- anions above/below the ring plane. On the other hand, all the other studied ILs show very similar distributions, centered between C^2 and N^3 with intensities following the order of $PF_6^- > BF_4^- \approx TfO^- > TFSA^- \geq Cl^-$.

The obtained trend is in excellent agreement with numerous results on related systems. The examples include MD simulations of Hardacre *et al.* aimed at reproducing neutron diffraction data on C_1mimCl/PF_6/TFSA and C_2mimOAc,[56, 62-66] as well as NMR, classical MD simulations and static *ab initio* calculations on ion pair dimers performed by Matthews *et al.* on C_1mimCl/TfO/NO_3/BF_4/$MeSO_4$ and C_4mimCl/TfO/SCN/TFSA/Me_2PO_4.[10-11] These results were, however, mainly based on the calculation of conventional SDFs with an arbitrary isovalues. The conclusions can be typically summarized as follows: the bigger and the less coordinating (H-bond accepting) the anion is, the more it prefers to occupy the above/below C-H^2 sites. A more quantitative assessment of this issue was given by Skarmoutsos *et al.*,[12] who reported a similar angular distribution for anions that are localized closer than the H-bonding distance at the C-H^2 site in C_4mimCl. Kirchner *et al.* reported the results of the relative arrangement of anions around cations, in a similar level of details as we presented here, on the basis of *ab initio* and classical MD simulations of C_2mim^+ coupled with cyano-based anions,[38] mixtures of C_2mimOAc with water,[58] neat C_4mimBr/I/OAc/CF_3COO/TFSA ILs,[39] and C_2mimCl-C_2mimSCN IL mixtures.[67] Nonetheless, their results mainly dealt with C-H^2 or CoR centered description. In the present work we present a particular level of structural details by considering nearest neighboring anions with respect to each relevant cation interaction site.

As for the nature of the interactions underlying the revealed structural motifs we first highlight that the present results are an outcome of a classical force-field and therefore conclusions are necessarily limited to the effects of size and charge distribution. Nonetheless, several static and dynamic *ab initio* studies have already tackled this question. It is assumed that the on-top arrangement of anions results from the so-called anion-π^+ interaction,[10-12, 68] which is a complex interplay of electrostatics and dispersion forces.[10-12, 38, 68]

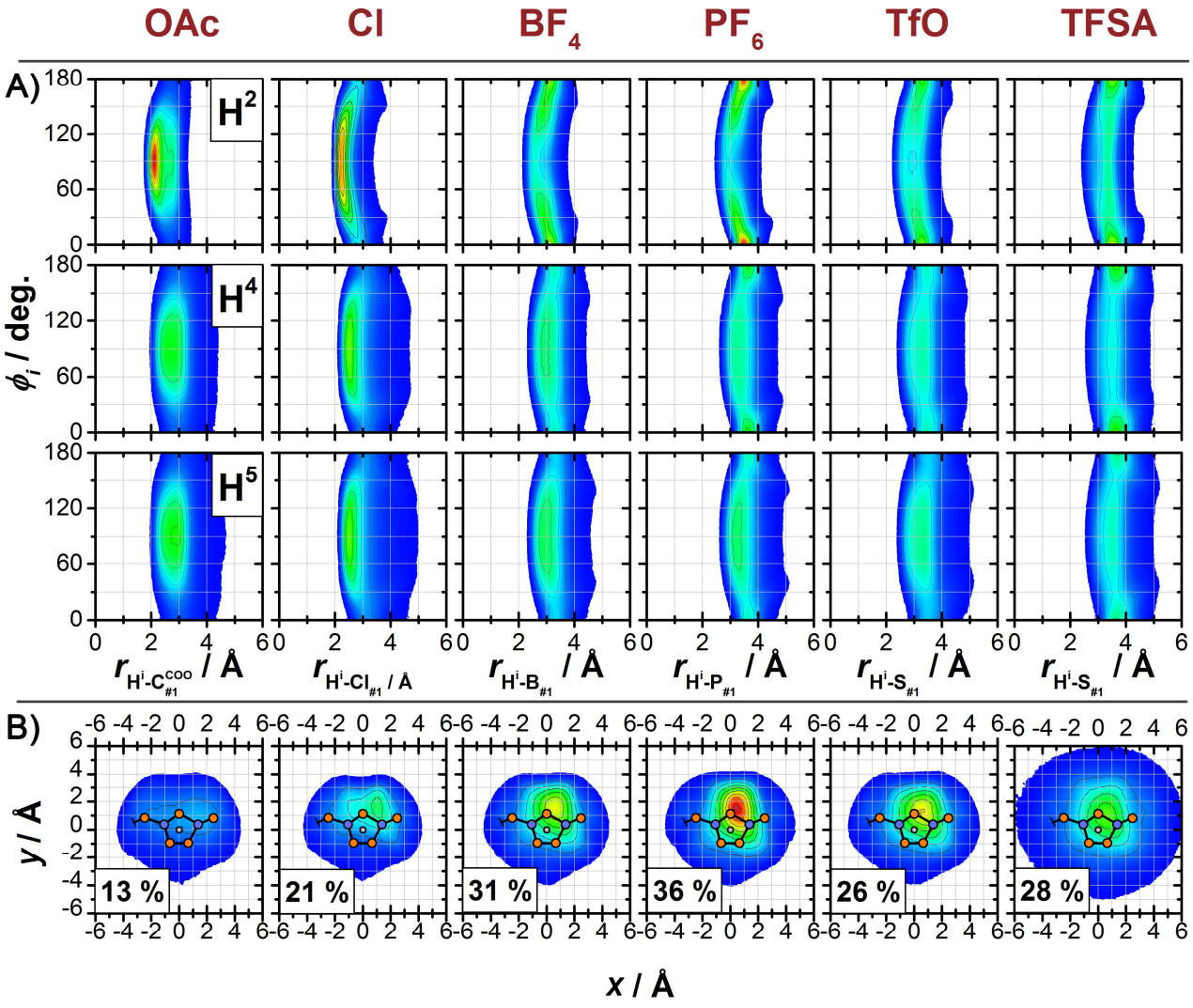

Figure 3. A) Combined distribution functions relating the distance of the vector connecting the imidazolium ring hydrogen sites H^2 (*top row*), H^4 (*middle row*), H^5 (*bottom row*) of C_4mim^+ cation and

the nearest central atom of coordinating group of anions and the angle between this angle and the normal to the imidazolium ring plane (φ). B) Contour plots of the density of projections on the imidazolium ring plane of the nearest to the CoR anions that are at the same time *not* the nearest neighbors of any of $H^{2/4-5}$ sites. The projection plane is centered at the CoR (grey circle) and part of the skeleton of a reference C_4mim^+ is shown for clarity. The percentages indicate the fraction of the nearest to the CoR anions that satisfy the second condition, *i.e.*, which are not the nearest neighbors of any of $H^{2/4-5}$. Color scaling range is different in A and B, but the same for all the studied ILs and reference sites.

3.2. Cation-anion H-bond-like interactions

It is well appreciated in the literature that, apart from the strong non-directional electrostatic interactions between the ions as charged entities, the local microscopic structure in imidazolium ILs is significantly influenced also by directional cation-anion H-bonding, though the extent and the importance of this contribution to the overall potential energy landscape is still under debate.[12, 15, 19, 37, 69-70] Within the framework of modern all-atom force fields this type of interaction is treated via coulombic terms and the corresponding atomic charges. The issue of cation-anion H-bonding in ILs has mainly been assessed by computer simulations studies using a certain H-bond criterion. Typically, this implies a combination of a radial cut-off between a given hydrogen atom and the corresponding H-bond acceptor, and an angular cut-off for the pseudovalent H-bond angle (D-H···A, where D and A stand for the H-bond donor and acceptor site, respectively).[71] However, in some studies more sophisticated criteria have also been used.[12] Moreover, some authors claim that poorly selected cut-off values can significantly bias the results,[12] while others stipulate that these results are rather insensitive to the cut-off values.[37]

In order to avoid this ambiguity in the present study we refrain from any H-bonding criteria and study rather H-bond-like interactions. We present in Figure 4 CDFs correlating the H-bond pseudovalent angle and the corresponding H-bonding distance between the imidazolium ring hydrogen atoms H^i and the

nearest neighboring H-bond accepting atom of anion (O in OAc^-, TfO^-, and $TFSA^-$, F in BF_4^- and PF_6^-, and Cl^-). Similarly to the general distribution of anions around the ring sites discussed before, several apparent features are common for all the studied ILs here. Namely, both angular and radial distributions are more diffuse at H^{4-5} than at H^2. Also, the preference of the H-bonds for the linear alignment is stronger around H^5 than H^4.

As for the IL-specific observations on cation-anion H-bonding at the imidazolium ring sites, one should mention that the relative strength of H-bonds estimated from their linearity/length follows the order OAc^- >> TfO^- > BF_4^- > $TFSA^-$ ≈ PF_6^-. C_4mimCl, the only IL considered that has a monoatomic anion, represents a rather particular case. Despite the fact that the main peaks are located at H-bonding distances, very close to linear arrangements and with intensities comparable to those of C_4mimTfO, one also sees broad low intensity features reaching rather large distances and low angle values. The latter originate from the above/below arrangements of the nearest neighboring anion which are also important as can be judged from Figure 3.

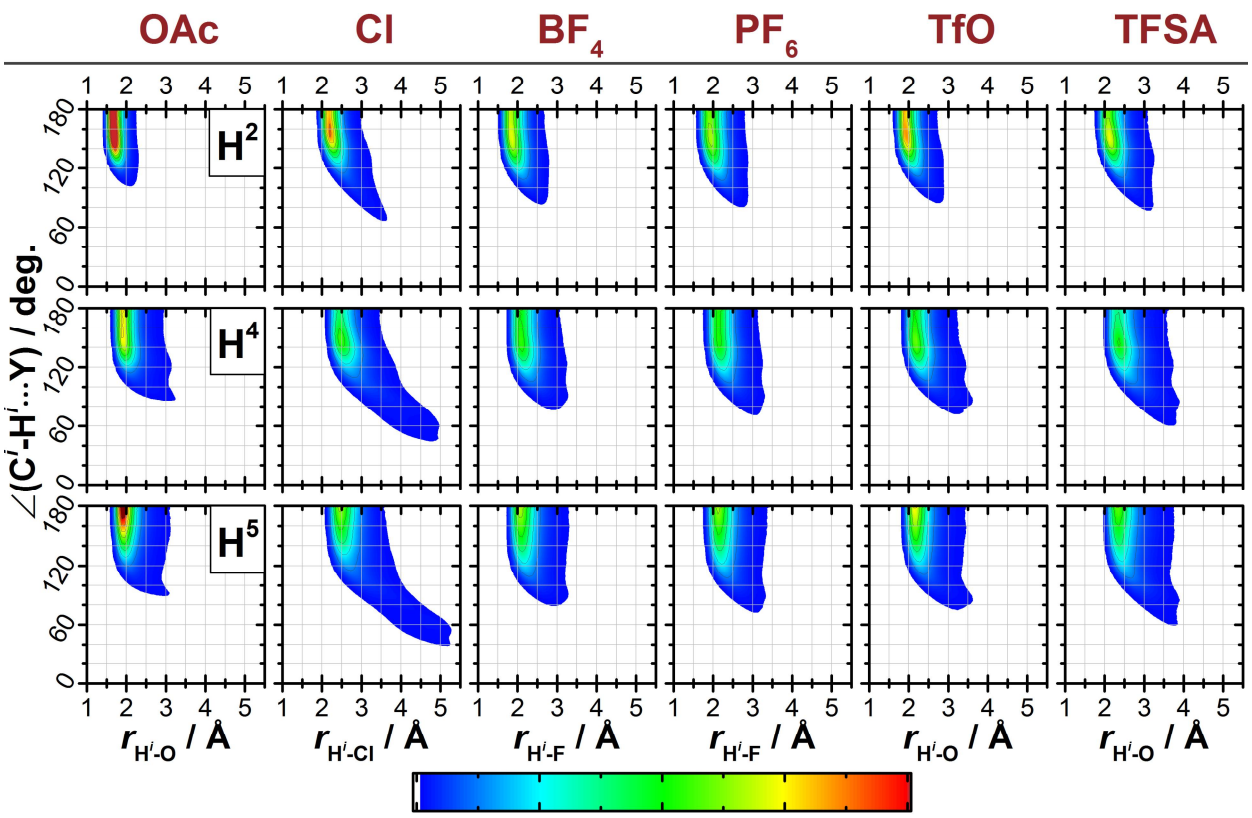

Figure 4. Combined distribution functions relating the distance and the corresponding pseudovalent angle of H-bond like interactions between the imidazolium ring hydrogen atoms H^2 (*top row*), H^4 (*middle row*), H^5 (*bottom row*) of the C_4mim^+ cation and the nearest neighboring primary H-bond accepting atom of anion (O for OAc, TfO, and TFSA, F for BF_4 and PF_6).

In our recent NMR study on neat C_4mimBF_4, C_4mimPF_6, $C_4mimTfO$, and $C_4mimTFSA$ and their mixtures with acetonitrile over a broad concentration range,[17] apart from the relative strength of cation-anion H-bonding in these ILs we also obtained an interesting result concerning the relative strength of H-bonds at the H^2 and H^{4-5} sites. In particular, it was established that H-bonding at H^2 is much stronger than at H^{4-5} in $C_4mimTfO$ and $C_4mimTFSA$, while this difference is less pronounced in C_4mimBF_4 and C_4mimPF_6. Given that the angular distribution of the H-bonding pseudovalent angle are quite similar in these ILs, we verify our experimental finding by calculating the average H-bond-like distance with the first nearest neighbor for each imidazolium ring site (Figure 5). It is readily apparent that the difference in

the average distances at H^2 and H^{4-5} is larger in the case of C_4mimTfO and C_4mimTFSA as compared to C_4mimBF_4 and C_4mimPF_6. The MD results are in accordance with our experimental findings, and also partly supported by another of our recent work on quantum-chemical calculations of ion pair dimers of these ILs.[18]

One of the main experimental evidences obtained by us in this regard was the IR bandshape of the stretching vibration of the imidazolium C-H^i bonds, namely the particularly strong low frequency shoulder corresponding to the C-H^2 stretching vibration.[17] The results presented in Figure 5 suggest that C_4mimCl and C_4mimOAc also reveal significantly enhanced H-bonding strength at H^2 similar to that found in C_4mimTfO and C_4mimTFSA. In accordance with this result, the published IR spectra of C_4mimCl[72-73] and C_4mimOAc[22] also show an intense redshifted band related to the C-H^2 stretching.

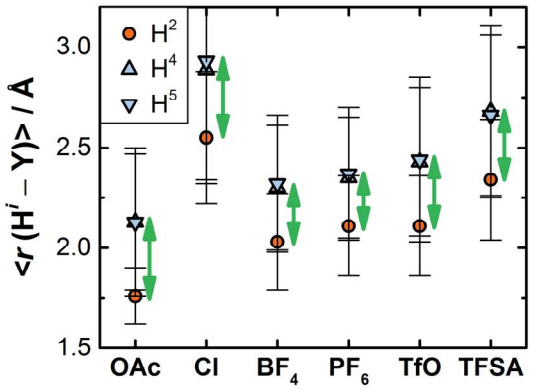

Figure 5. Average distance between the imidazolium ring hydrogen atoms H^2, H^4, H^5 of C_4mim^+ cation and the nearest neighboring primary H-bond accepting atom of anion (O for OAc, TfO, and TFSA, F for BF_4 and PF_6). The error bars are an estimation of the corresponding fluctuation of the average distance. Double-headed green arrows serve to mark the difference between the average values for H^2 and H^{4-5}.

All the anions considered in this study, with the exception of Cl^-, can form multiple H-bonds with a given hydrogen atom. This point has mainly been studied in acetate-based systems,[56, 58] however, numerous static quantum-chemical calculations on representative ion pair clusters suggest that this issue is also

important in ILs with perfluorinated anions.[15, 18, 74] As we stick to the idea of the nearest neighbor approach, and try to avoid the use of any arbitrary H-bonding criteria, here we propose to follow the correlations between the distances from a given ring hydrogen atom to H-bond accepting atoms of the nearest neighboring anion. The nearest neighboring anion here was defined with respect to the distance between the ring hydrogen atoms $H^{2/4-5}$ and the central atom of the coordinating group of the anion (see above). The obtained CDFs are shown in Figure 6. The simplest case is C_4mimOAc, because here the anion has only two oxygen atoms, and thus, the leftmost column of Figure 6 contains the CDFs correlating the distances $H^{2/4-5}$-$O^{1/2}$. In this representation a bidentate coordination of the OAc^- anion to a given hydrogen atom would correspond to a cross-peak at the diagonal, where both H^i-$O^{1/2}$ distances are short, whereas a monodentate motif should give rise to two contributions where one distance is H-bond-like and the other one is larger.

However, as the other anions have at least three atoms that could possibly simultaneously coordinate a given hydrogen atom, the visualization of such multidimensional data is rather complicated. In order to simplify the representation, we analyzed only those nearest neighboring anions that have one H-bond with a given hydrogen atom. This was realized by applying a condition that the distance from a given hydrogen atom to an H-bond accepting atom of the nearest neighboring anion is within the standard deviation from the average position of the first nearest neighbor of this type, in other words, within the limits of the appropriate error bars in Figure 5. Then, after selecting the configurations that fit these conditions, we analyze the CDFs of the distances from the selected hydrogen atom to two other H-bond accepting atoms of the nearest neighboring anion that were not considered in the above condition. In other words, these CDFs, presented in columns 2 to 5 of Figure 6, correspond to an observation of two different atoms (a three-body analysis) with a condition applied to a third one.

Within this framework a monodentate coordination means that only the first H-bond accepting atom of the nearest neighboring anion, *i.e.*, the one that served for the condition, is within the typical H-bonding

distance from a given hydrogen atom. In other words, in the CDFs shown in columns 2-5 of Figure 6 such configurations would contribute to the probability density corresponding to high values of both observed distances. Similarly, a bidentate coordination implies that apart from the first H-bond accepting atom, one of the two others should be observed at short, H-bonding-like distances, while the other one is much farther from the given hydrogen atom. Finally, a tridentate coordination would give rise to a cross-peak along the diagonal at short distances (*i.e.*, an equivalent of the bidentate coordination pattern for OAc^-). For this set of systems, we highlight the range of H-bonding distances used in the criteria for the first H-bond accepting atom with hatched squares in Figure 6.

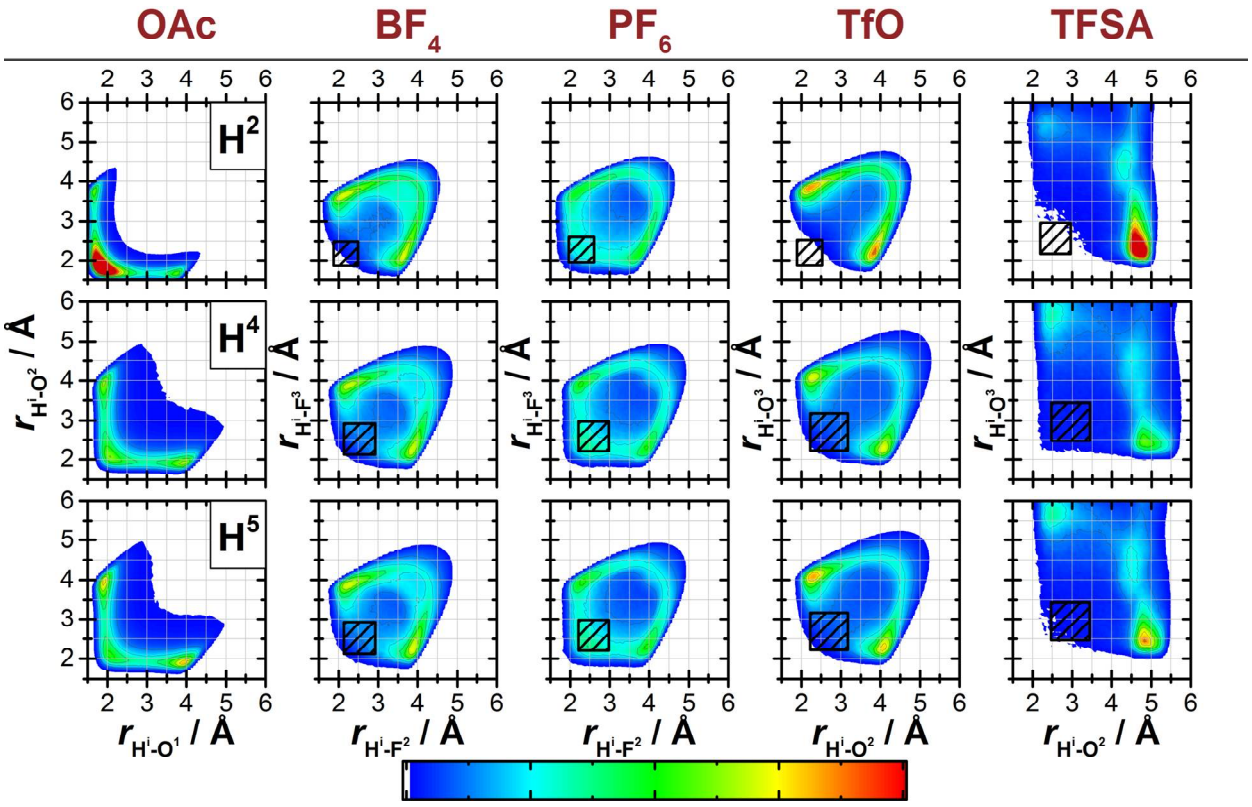

Figure 6. Combined distribution functions relating the distances from H^2 (*top row*), H^4 (*middle row*), H^5 (*bottom row*) of C_4mim^+ cation to the two oxygen atoms of the nearest OAc anion (*1st column*) or to two different H-bond accepting atoms of the nearest anion (O for TfO, and TFSA, F for BF_4 and PF_6) under the condition that a third atom is within a certain distance condition as explained in the text (*columns 2 to*

5). The hatched square in CDFs shown in columns 2 to 5 encloses the range of distances used as the criterion applied to the third (not-observed) H-bond accepting atom.

We begin this analysis with C_4mimOAc, whose anion can only be mono- or bidentate. From Figure 6 it is evident that the bidentate mode of coordination is strongly dominating at the C-H^2 site due to its highly positive charge. However, at C-H^4 and, to a greater extent, at C-H^5 we observe a slight preference for the monodentate coordination of OAc^- anions. This preference can be explained by the larger sterical hindrance around these H atoms. It also worth mentioning that the transition from a monodentate to bidentate H-bonding mode goes through a minimum of probability where the longer of the two distances is around 3 Å. This means that if necessary one could easily distinguish between the different coordination patterns. However, Bowron *et al.*[56] claimed on the basis of direct MD simulations and EPSR refinement of neutron diffraction data of C_2mimOAc that bidentate binding of the anion is of low probability even at the C-H^2 site. One has to remark though that they analyzed all ion pairs within the first minimum of the corresponding H^i-O^{OAc} RDFs, not just the nearest neighboring ones, as done here.

C_4mimBF_4, C_4mimPF_6, and C_4mimTfO are different from C_4mimOAc as their anions can potentially form up to three H-bonds with a given hydrogen atom using three equivalent H-bond accepting atoms. As one can see from Figure 6, several observations are universally applicable to all the three ring sites in this set of ILs. First, the most probable H-bonding mode is the bidentate one, as indicated by the large peaks (at 2.0-2.5 Å / 3.5-4.5 Å) located symmetrically at the two sides of the diagonal. Second, tridentate configurations are more probable at $H^{4\text{-}5}$ sites than at H^2 (note the higher intensity close to the hatched regions in the case of $H^{4\text{-}5}$ as compared to H^2). Finally, transition from the dominating bidentate configuration to either a monodentate or the tridentate one passes through a monotonic decrease of probability. This is in a clear contrast to what has been seen for C_4mimOAc, as less probable H-bonding modes do not correspond to local maxima on the probability density maps shown in Figure 6, which makes quantitative distinguishing between different H-bonding coordination patterns rather ambiguous. It

is also worth noting that the stable ion pair geometries of C_4mimBF_4, C_4mimPF_6, and $C_4mimTfO$,[18] reported previously by us, revealing that the anion is located above the C-H^2 fragment, are fully compatible with the prevailing bidentate H-bonding mode revealed here.

As for IL specific features of multiple H-bonding of a given ring C-H site with the nearest anion, we note a significant population of the tridentate arrangement, comparable to that of the monodentate one, in the case of C_4mimPF_6. In C_4mimBF_4 and $C_4mimTfO$ the tridentate H-bonding occurs less frequently than the monodentate one. Among these two ILs, it is C_4mimBF_4 that exhibits more tridentate H-bonding. In other words, the average number of close H-bond like contacts with the nearest neighboring anion follows the order C_4mimPF_6 > C_4mimBF_4 > $C_4mimTfO$.

Lastly, we describe the multiple H-bonding with the nearest $TFSA^-$ anion. Here the two H-bond like distances, analyzed in Figure 6, refer to two non-equivalent oxygen atoms. Namely, the distance corresponding to the horizontal axis of the graph is that to the O^2 oxygen atom, which resides in the same SO_2 moiety as the O^1 oxygen atom used for defining the condition. Accordingly, the distance plotted along the vertical axis is that to the O^3 oxygen atom, corresponding to the other SO_2 group. The main peak at 4.5 Å / 2.5 Å implies a very strong preference, particularly at the C-H^2 site, for the bidentate H-bonding between oxygen atoms of two different SO_2 groups. Nevertheless, weak populations of monodentate and bidentate configurations within the same SO_2 group are also apparent. Similarly to C_4mimBF_4 and $C_4mimTfO$, tridentate configurations are hardly observed at the C-H^2 site, while they are encountered at $H^{4\text{-}5}$ though with a very low probability.

Our final insight into cation-anion H-bonding concerns such non-conventional H-bond donors as aliphatic C-H sites of the butyl and methyl groups of C_4mim^+ cation. It has been often acknowledged in molecular modeling studies[11-12, 15, 18, 68, 74] that anions located close to the imidazolium ring C-H sites can also establish slightly weaker H-bonds with the adjacent alkyl hydrogen atoms of the alkyl chains. This claim

has been experimentally confirmed in neat ILs via the isotopic shift of ^{19}F NMR signals after selective deuteration of the C_4mim^+ cation in C_4mimBF_4 and C_4mimPF_6,[75] and also in their solutions in various molecular solvents, from concentration dependent chemical shifts.[17, 22-23]

Similarly to Figure 4, we present in Figure 7 the CDFs relating the H-bonding distance and the corresponding pseudovalent angle between different alkyl hydrogen atoms of the C_4mim^+ cation and the nearest neighboring H-bond accepting atom of the anions. Not surprisingly, the H-bonds involving the alkyl hydrogen atoms are less frequent (note the scale used in Figure 7 is half of that in Figure 4), longer, and deviate more from the linear arrangement than those involving the imidazolium ring C-H sites. The fact that the distributions are the least diffuse for the $H^{\alpha'}$ site can be traced back to the better special accessibility of this H atom. Moreover, it can contribute to the cation-anion H-bonding not only in configurations where anion is simultaneously bound to H^2 or H^4 of the same C_4mim^+ cation, but also in configurations in which the anion is located directly in front of the N^3-$C^{\alpha'}H_3$ group, as indicated by a weak probability zone of the cross-sections shown in Figure S3. This finding supports the importance of $H^{\alpha/\alpha'}$ hydrogen atoms not only in the analysis of the cation-anion interactions in ILs, but in the force-field development as well.[12, 57]

In general, the H-bonds with hydrogen atoms of the butyl chain become progressively weaker as one gets farther away from the imidazolium ring. The only obvious exception here is C_4mimPF_6, as it reveals rather equally strong H-bonds with all types of alkyl hydrogen atoms along the butyl chain of the C_4mim^+ cation. This finding can be related to the well defined localization of the PF_6^- anion above/below the C-H^2 site, and could be one of the reasons of its surprisingly high viscosity of *ca*. 280 mPa s.[76]

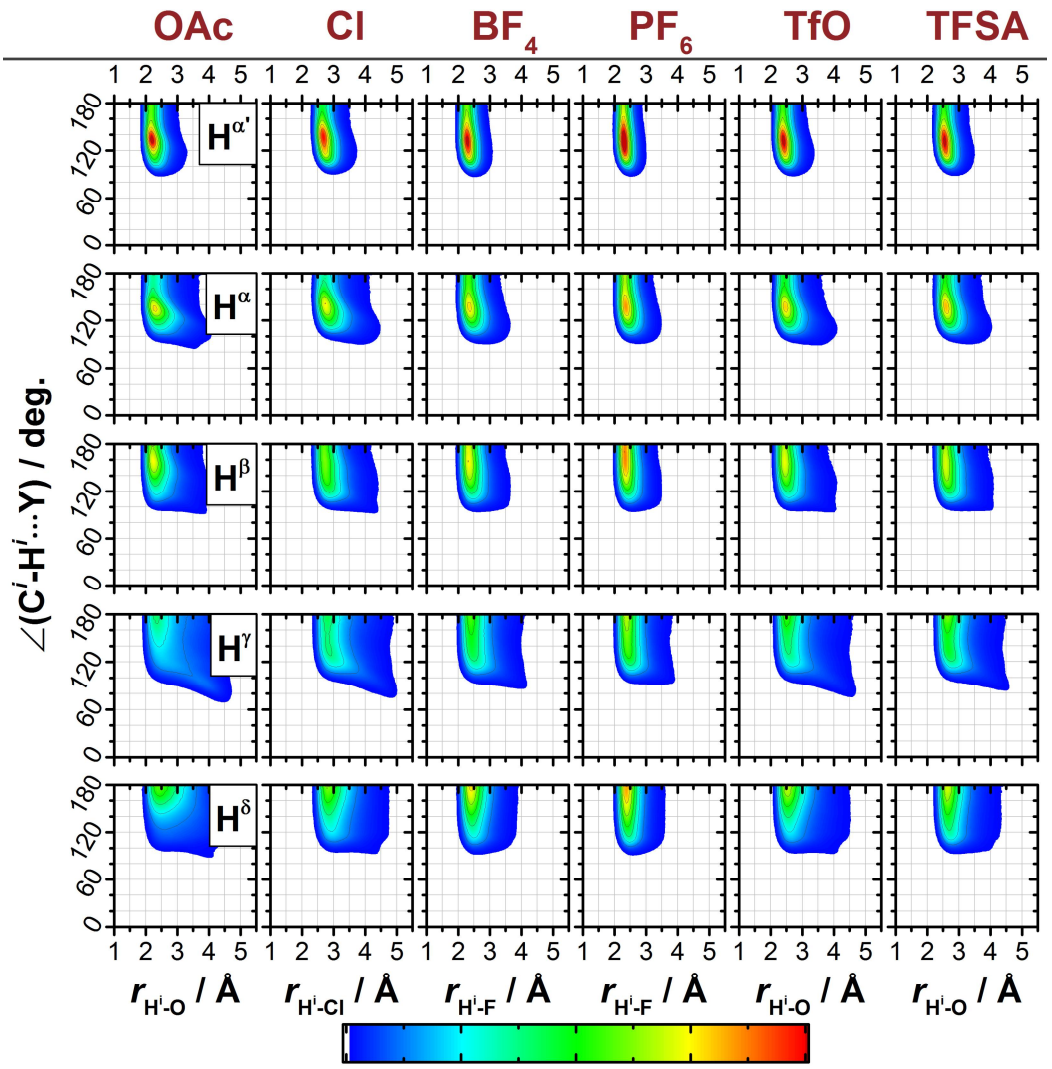

Figure 7. Combined distribution functions relating the distance and the corresponding pseudovalent angle of H-bond-like interactions between the alkyl hydrogen atoms of C_4mim^+ cation and the nearest neighboring primary H-bond accepting atom of anion (O for OAc, TfO, and TFSA, F for BF_4 and PF_6). Intensity scale is twice as small as in Figure 4.

3.2. Cation-cation arrangement

Despite the fact that the local environment of cations in imidazolium-based ILs is mainly determined by the surrounding counterions it is well understood that cation-cation contacts also play significant role in determining the properties of the corresponding IL. Two typical kinds of contacts have been reported in

imidazolium-based ILs: tail-tail and ring-ring (*e.g.*, π^+-π^+ stacking).[1, 11, 39, 74] The former one is known to be at the origin of microheterogeneity observed both experimentally[1, 77-78] and by molecular simulations.[3, 27-28] The latter, by contrast, is much less common and was initially suggested to rationalize some NMR spectroscopic data,[79-81] and was also confirmed later by MD simulations, including ones that well reproduce neutron and X-ray scattering data.[4, 62, 66]

It is interesting to note that in the available experimental crystal structures of C_4mim^+-based ILs, among which several ones are studied here, no stacking type close contacts were observed, though the neighboring ring planes are often, but not always, parallel and displaced.[82-83] Several recent quantum-chemical calculations on representative clusters of ion pairs of C_4mim^+-based ILs have also revealed the importance of π^+-π^+ stacking in such systems.[10-11, 18, 68, 74, 84-86]

We address here these two types of cation-cation contacts through conventional RDFs (Figure 8) between the centers of imidazolium rings (CoR), and between the terminal carbon atoms of the butyl chain (C^δ). It is readily apparent that the chain-chain aggregation is much less IL specific, though it is obviously stronger than the π^+-π^+ stacking. The first peak in the C^δ – C^δ RDFs is located at 4 Å with a distinct shoulder at *ca.* 5 Å. The main peak accommodates approximately one neighbor, whereas integration up to the first minimum located at 6.5-7 Å gives around 3-3.5 neighbors, except for C_4mimTFSA, for which the coordination number is close to 2 due to the bulkiness of the anion. The second shell of chain-chain contacts is hardly discernable.

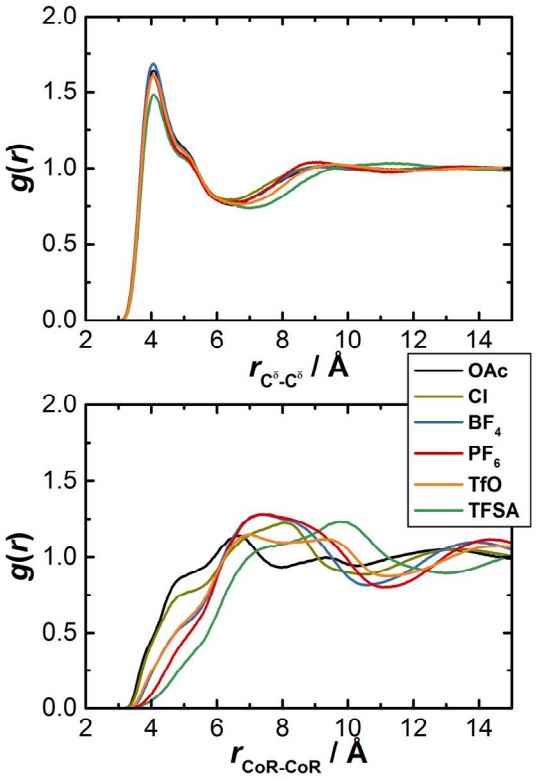

Figure 8. Radial distribution functions relating two main types of cation-cation aggregation: between the butyl chains (*top*) and between the imidazolium rings (*bottom*).

As already mentioned before, the CoR-CoR distributions are much more complex and sensitive to the type of anion. First, none of these distributions exhibits a distinct sharp first peak. Instead, one can observe a series of shoulders and humps with a complicated structure. Second, the initial slope of the curve corresponding to stacking contributions at 3-4 Å follows the order of $OAc^- \approx Cl^- > BF_4^- \approx TfO^- > PF_6^- > TFSA^-$. This trend only represents the general tendency for stacking. In order to resolve the orientational aspects of this interaction, we study several angular distributions (see Figure 9) for the first nearest neighbor with respect to the CoR-CoR distance. The results are presented in Figure 10 as CDFs correlating one of the selected angles and the distance between the centers of two closest imidazolium rings.

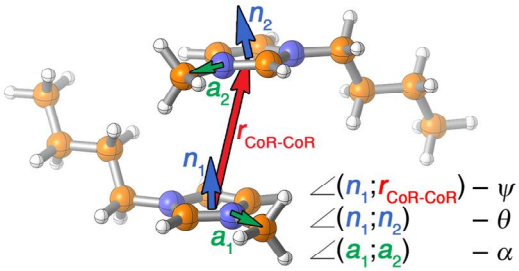

Figure 9. Schematic representation of the parameters used to description of the relative orientation of two C_4mim^+ cations.

The first investigated angle, designated here as ψ, is the angle between the normal vector of the imidazolium ring plane of the reference C_4mim^+ cation and the vector connecting the ring centers of the reference cation and the observed nearest neighboring C_4mim^+ cations. This angle is analogous to the φ angle that we used to describe the relative position of anions with respect to cations. If the center of the imidazolium ring of the observed cation is located exactly above/below that of the reference one, it will contribute to at ψ values close to 0 and 180°. Similarly, an in-plane arrangement of the observed nearest neighboring cation corresponds to a ψ value around 90°. One can clearly see from Figure 10 that in all the investigated ILs the nearest neighboring cation prefers to occupy the above/below positions at typical stacking distances around 3.5-4.5 Å. Noteworthy, this preference is much weaker for C_4mimPF_6 and $C_4mimTFSA$ than for the other ILs considered, and the corresponding peaks are much broader along the radial variable and are shifted to longer distances.

Stacking interactions including those in imidazolium-based ILs[39, 87-88] imply not only good relative above/below arrangement of the interacting planes, but also their essentially parallel relative arrangement. This is characterized here by the angle θ formed by the normal vectors of the imidazolium ring planes of the reference and observed molecules. Again, a perfectly parallel arrangement of the planes corresponds to θ values of 0 or 180°, whereas the values around 90° are indicative of T-shaped relative arrangement of the two rings. For all the ILs studied here (with the exception of $C_4mimTFSA$, which does not show any distinct preferences for stacking), we observe a strong bias towards parallel alignment of the imidazolium

ring planes of the first nearest neighboring cation. This preference is even somewhat stronger than that for the above/below arrangement. In other words the angular distribution peak of ψ is broader than that of θ.

So far, we have established that the nearest neighboring cation ring prefers parallel stacking and direct above/below arrangement relative to the reference one, although some displacement from this perfect alignment is also possible. C_4mimOAc and C_4mimCl, *i.e.*, the ILs with the strongest preference for the in-plane arrangement of anions at all the ring sites, reveal the most favorable stacking alignments of the cations. Conversely, C_4mimPF_6 and C_4mimTFSA exhibit hardly any particular stacking type arrangements due to the preferential localization of anions above/below the ring plane, and to their large size (in particular, for C_4mimTFSA). C_4mimBF_4 and C_4mimTfO constitute an intermediate case of π^+-π^+ stacking. It should be reminded, however, that the present results are obtained from classical MD simulations, *i.e.*, they stem from merely point-charge electrostatics and molecular packing considerations, while quantum-chemical treatment of π^+-π^+ interactions are out of scope here. Static quantum chemical calculations on a set of ion pair dimers of C_1mim$^+$-based ILs, reported recently by Matthews *et al.*[74] also highlighted the tendency of multidentate big anions to prefer the on-top arrangement, thus preventing cations from stacking. In their subsequent combined NMR/MD study on mixtures of C_4mim$^+$-based ILs with different anions they reinforced their findings that smaller anions, showing higher H-bond accepting capacity can stabilize π^+-π^+ stacking, whereas bulky anions with diffuse charge distribution favor the anion- π^+ interactions.[10] However, a very recent *ab initio* MD study of C_2mim$^+$-based ILs with cyano-bearing anions by Weber and Kirchner [38] suggests that cation stacking and on-top anion arrangement are not always in direct competition.

One can also get an idea about the relative orientation of two stacked imidazolium rings by following the angle α (Figure 9), which is the angle between the vectors N^3-$C^{\alpha'}$ in the reference and observed C_4mim$^+$ cations. Orientations in which the equivalent alkyl groups point to the same direction correspond to the α

values of 0°. It is apparent from the bottom row in Figure 10 that the four ILs are prone to stack with equal preferences for parallel and anti-parallel arrangements of the alkyl groups.

Brehm *et al.* inferred from small but still representative *ab initio* MD simulations of neat C_2mimOAc and its mixtures with water[58] that the alkyl chains of the nearest neighboring cations in the corresponding stacking arrangement (*on top* and parallel with respect to the reference one) are oriented in an orthogonal fashion. On the one hand, this result could stem from the better description of the manifold of interactions between the ions in *ab initio* MD compared to the classical MD used in the present study. On the other hand, in the case of C_4mim^+-based ILs one would naturally expect stronger bias towards (anti)parallel arrangement of the alkyl chains due to packing restrictions and aggregation of the nonpolar moieties. Moreover, many published to date structures of quantum chemically optimized ion pair clusters of C_4mim^+-based ILs[18, 84, 86] reveal collinear arrangement of the butyl chains.

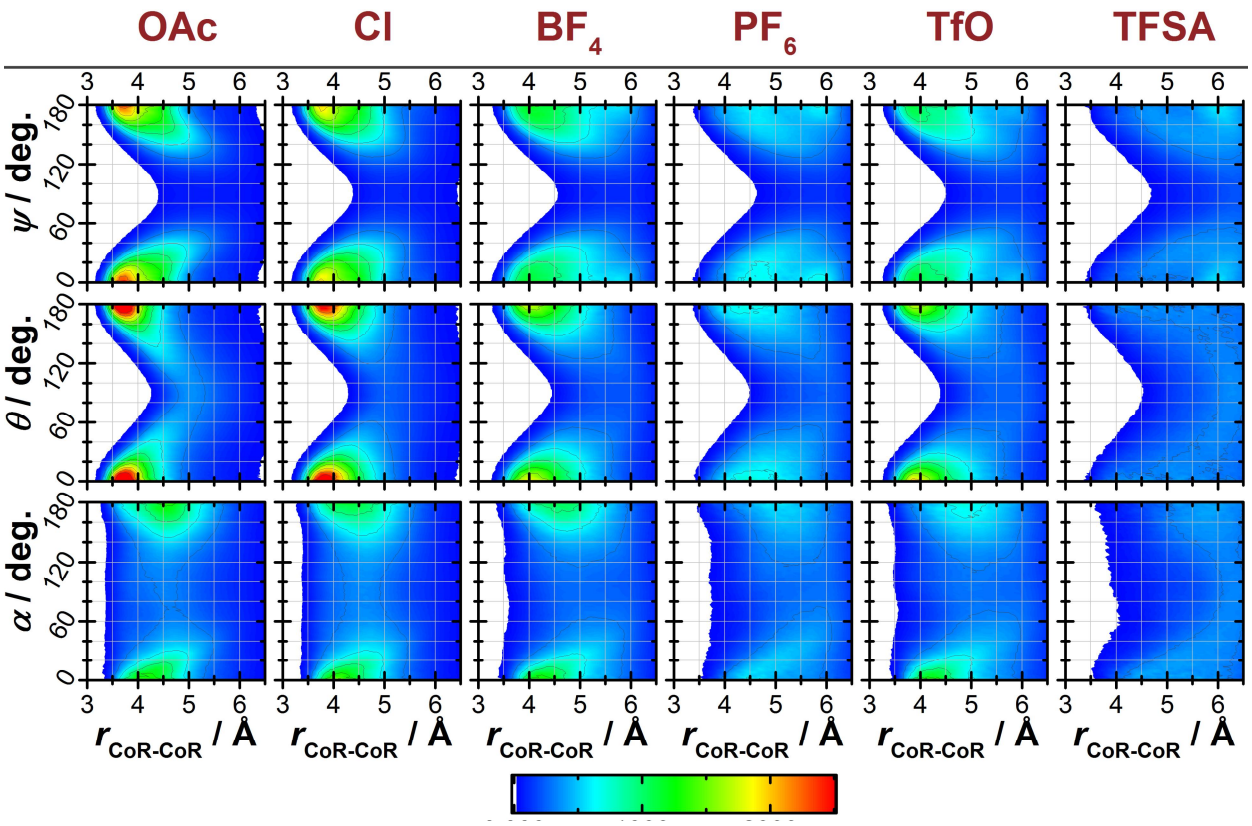

Figure 10. Combined distribution functions relating the 1st nearest neighbor CoR-CoR distance between two C_4mim^+ cations and the three representative angles ψ (*top row*), θ (*middle row*), and α (*bottom row*) reporting their relative orientation.

The latter observation highlights the fact that the ring stacking of cations can occur simultaneously with the aggregation of the butyl chains. In order to study this aspect more precisely we present in Figure 11 the CDFs correlating the C^δ – C^δ and CoR – CoR distances under two alternative conditions. The first one implies that the observed cation is the nearest neighbor with respect to the distance between the terminal carbon atoms C^δ of the butyl chain, whilst the second condition applied refers to the nearest neighbor with respect to the CoR-CoR distance. The results suggest that if two neighboring C_4mim^+ cations are aggregated via their butyl chain, the most probable distance between the centers of their imidazolium rings is around 6.5 Å in C_4mimOAc, and around 7.5-8.0 Å in the other ILs studied. Nevertheless, in C_4mimCl and C_4mimOAc one observes a non-negligible contribution as a secondary peak/shoulder at the higher limit of stacking distances around 4.5 Å. This means that in the case of the butyl chain aggregation

between a pair of C_4mim^+ cations the π^+-π^+ stacking between the same cations is only essential in ILs that show a strong tendency to the imidazolium ring stacking, *e.g.*, C_4mimCl and C_4mimOAc. Similar results were reported by Weber *et al.*[39] for a similar set of C_4mim^+-based ILs.

In the opposite case, *i.e.*, when one considers a pair of stacked C_4mim^+ cations the distribution of distances between the terminal carbon atoms of the butyl chains is rather broad and featureless within the range of 4-8 Å, peaking at 4 Å. In other words, in the studied ILs, the stacking of cations does not impose any particular arrangement between their corresponding butyl chains.

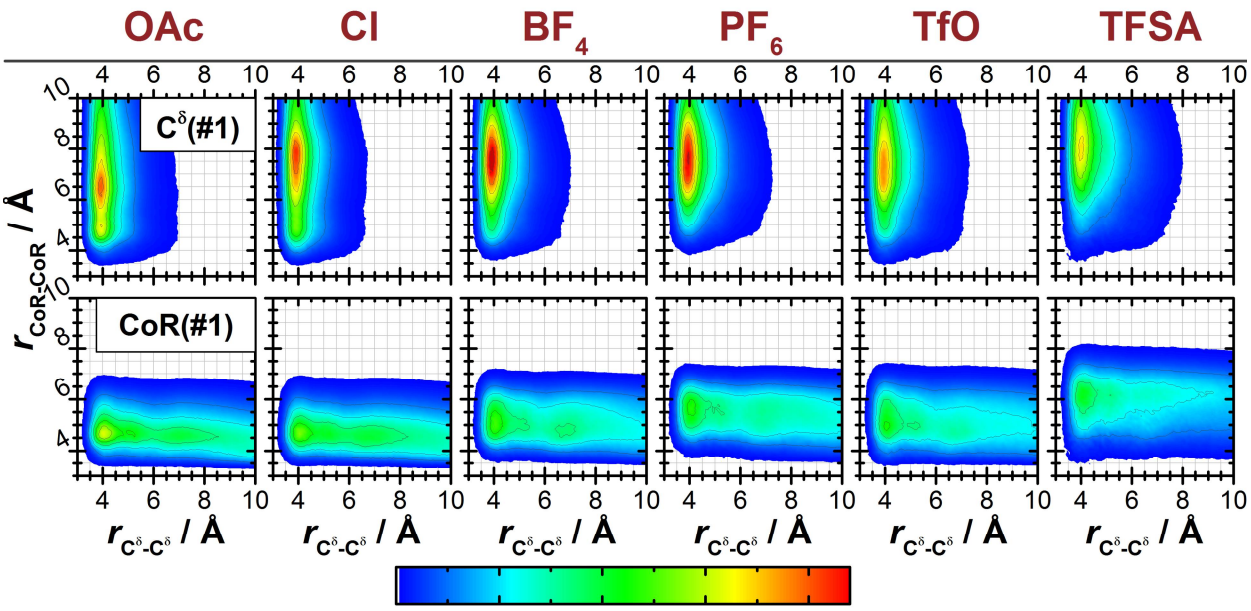

Figure 11. Combined distribution functions relating the distance between the terminal carbon atoms C^δ and the distance between the centers of rings (CoR) for a pair of closest C_4mim^+ cations with respect to their C^δ (*top row*) or their CoR (*bottom row*).

4. Conclusions

We have studied site-specific nearest neighboring local environment of cations in six ionic liquids bearing C_4mim^+ cation coupled with OAc^-, Cl^-, BF_4^-, PF_6^-, TfO^-, and $TFSA^-$ anions by means of classical MD simulations. Particular attention was paid to the issues of the influence of the nature of anion on the

relative cation-anion and cation-cation localization as well as on cation-anion H-bonding in terms of radial and orientational distributions of the nearest neighbors.

The results suggest that the position of the anion with respect to the imidazolium ring plane of the cation is strongly anion-dependent, especially around the C-H^2 site. Namely, OAc^- and Cl^- anions strongly prefer to occupy the in-plane position, while the other anions studied tend to the on-top arrangement. The corresponding distribution at the C-H^{4-5} sites is much more diffuse.

H-bonding at the H^2 site is strongly enhanced as compared to the H^{4-5} sites in the case of asymmetric and/or strongly basic anions, such as OAc^-, Cl^-, TfO^- or $TFSA^-$. This finding is also in accordance with recent spectroscopic and theoretical claims.[10, 17-18] Multiple H-bonding (bi- and even tri-dentate, when possible) with the nearest neighboring anion was observed to be prevailing at the H^{4-5} sites as compared to the H^2 one in all the ILs with multiatomic anions, except for C_4mimOAc. H-bonding like short contacts were also found between the anions and alkyl C-H groups in all the studied anions, though remarkably less frequent and directional than those involving ring hydrogen atoms.

Finally, cation-cation contacts via the aggregation of the butyl chains is found to be much stronger and less anion-dependent than the π^+-π^+ stacking of the imidazolium rings. The latter, however, can occur simultaneously with the alkyl chain aggregation, particularly in the case of ILs whose anions tend to be located in the imidazolium ring plane and hence do not hamper the stacking, such as C_4mimOAc and C_4mimCl.

Supporting information

Dihedral potential parameters refitted in accordance with eq. 1, densities of the simulated systems and cation-anion radial distribution functions (RDFs).

Acknowledgemetns

The Centre de Ressources Informatiques (CRI) de l'Université de Lille and Centre Régional Informatique et d'Applications Numériques de Normandie (CRIANN) are thankfully acknowledged for the CPU time allocation. O.N.K. thankfully acknowledges financial support from the Ministry of Education and Science of Ukraine (grant No. 0115U000483). V.A.K. thanks Erasmus Mundus IANUS II program for the PhD grant. The study was partly supported by Dean's Grant for Progressive Research Projects from Saga University (Japan) allowing B.A.M., A.I., and T.T to discuss the results at Saga University. P.J. acknowledges financial support of NKFIH under project No. 119732.

References

1. Hayes, R.; Warr, G. G.; Atkin, R. Structure and Nanostructure in Ionic Liquids. *Chem. Rev.* **2015,** *115*, 6357-6426.
2. Plechkova, N. V.; Seddon Kenneth, R. *Ionic Liquids Completely Uncoiled: Critical Expert Overview*. John Wiley & Sons, Inc.: Hoboken, New Jersey, 2015; p 535.
3. Kirchner, B.; Hollóczki, O.; Canongia Lopes, J. N.; Pádua, A. A. H. Multiresolution Calculation of Ionic Liquids. *Wiley Interdiscip. Rev.: Comput. Mol. Sci.* **2015,** *5*, 202-214.
4. Zahn, S.; Brehm, M.; Brüssel, M.; Hollóczki, O.; Kohagen, M.; Lehmann, S.; Malberg, F.; Pensado, A. S.; Schöppke, M.; Weber, H.; Kirchner, B. Understanding Ionic Liquids from Theoretical Methods. *J. Mol. Liq.* **2014,** *192*, 71-76.
5. Kirchner, B. Ionic Liquids from Theoretical Investigations. In *Ionic Liquids*, Kirchner, B., Ed. Springer-Verlag: Berlin/Heidelberg, 2010; Vol. 290, pp 213-262.
6. Chaban, V. V.; Prezhdo, O. V. A New Force Field Model of 1-Butyl-3-Methylimidazolium Tetrafluoroborate Ionic Liquid and Acetonitrile Mixtures. *Phys. Chem. Chem. Phys.* **2011,** *13*, 19345-19354.
7. Chaban, V. Polarizability Versus Mobility: Atomistic Force Field for Ionic Liquids. *Phys. Chem. Chem. Phys.* **2011,** *13*, 16055-16062.
8. Mondal, A.; Balasubramanian, S. A Refined All-Atom Potential for Imidazolium-Based Room Temperature Ionic Liquids: Acetate, Dicyanamide, and Thiocyanate Anions. *J. Phys. Chem. B* **2015,** *119*, 11041-11051.
9. Mondal, A.; Balasubramanian, S. Quantitative Prediction of Physical Properties of Imidazolium Based Room Temperature Ionic Liquids through Determination of Condensed Phase Site Charges: A Refined Force Field. *J. Phys. Chem. B* **2014,** *118*, 3409-3422.
10. Matthews, R. P.; Villar Garcia, I. J.; Weber, C. C.; Griffith, J. A.; Cameron, F.; Hallett, J.; Hunt, P.; Welton, T. A Structural Investigation of Ionic Liquid Mixtures. *Phys. Chem. Chem. Phys.* **2016,** *18*, 8608-8624.
11. Matthews, R. P.; Welton, T.; Hunt, P. A. Competitive Pi Interactions and Hydrogen Bonding within Imidazolium Ionic Liquids. *Phys. Chem. Chem. Phys.* **2014,** *16*, 3238-3253.
12. Skarmoutsos, I.; Dellis, D.; Matthews, R. P.; Welton, T.; Hunt, P. A. Hydrogen Bonding in 1-Butyl- and 1-Ethyl-3-Methylimidazolium Chloride Ionic Liquids. *J. Phys. Chem. B* **2012,** *116*, 4921-4933.
13. Tsuzuki, S.; Tokuda, H.; Mikami, M. Theoretical Analysis of the Hydrogen Bond of Imidazolium C_2–H with Anions. *Phys. Chem. Chem. Phys.* **2007,** *9*, 4780-4784.

14. Tsuzuki, S.; Tokuda, H.; Hayamizu, K.; Watanabe, M. Magnitude and Directionality of Interaction in Ion Pairs of Ionic Liquids: Relationship with Ionic Conductivity. *J. Phys. Chem. B* **2005,** *109*, 16474-16481.
15. Hunt, P. A.; Ashworth, C. R.; Matthews, R. P. Hydrogen Bonding in Ionic Liquids. *Chem. Soc. Rev.* **2015,** *44*, 1257-1288.
16. Hunt, P. A.; Gould, I. R. Structural Characterization of the 1-Butyl-3-Methylimidazolium Chloride Ion Pair Using Ab Initio Methods. *J. Phys. Chem. A* **2006,** *110*, 2269-2282.
17. Marekha, B.; Kalugin, O.; Bria, M.; Idrissi, A. Probing Structural Patterns of Ion Association and Solvation in Mixtures of Imidazolium Ionic Liquids with Acetonitrile by Means of Relative ^{1}H and ^{13}C NMR Chemical Shifts. *Phys. Chem. Chem. Phys.* **2015,** *17*, 23183 - 23194.
18. Marekha, B. A.; Kalugin, O. N.; Idrissi, A. Non-Covalent Interactions in Ionic Liquid Ion Pairs and Ion Pair Dimers: A Quantum Chemical Calculation Analysis. *Phys. Chem. Chem. Phys.* **2015,** *17*, 16846-16857.
19. Zahn, S.; Bruns, G.; Thar, J.; Kirchner, B. What Keeps Ionic Liquids in Flow? *Phys. Chem. Chem. Phys.* **2008,** *10*, 6921-6924.
20. Chaban, V. V.; Prezhdo, O. V. Ionic and Molecular Liquids: Working Together for Robust Engineering. *J. Phys. Chem. Lett.* **2013,** *4*, 1423-1431.
21. Dommert, F.; Wendler, K.; Berger, R.; Delle Site, L.; Holm, C. Force Fields for Studying the Structure and Dynamics of Ionic Liquids: A Critical Review of Recent Developments. *ChemPhysChem* **2012,** *13*, 1625-1637.
22. Marekha, B. A.; Bria, M.; Moreau, M.; De Waele, I.; Miannay, F.-A.; Smortsova, Y.; Takamuku, T.; Kalugin, O. N.; Kiselev, M.; Idrissi, A. Intermolecular Interactions in Mixtures of 1-N-Butyl-3-Methylimidazolium Acetate and Water: Insights from Ir, Raman, Nmr Spectroscopy and Quantum Chemistry Calculations. *J. Mol. Liq.* **2015,** *210, Part B*, 227-237.
23. Takamuku, T.; Hoke, H.; Idrissi, A.; Marekha, B. A.; Moreau, M.; Honda, Y.; Umecky, T.; Shimomura, T. Microscopic Interactions of the Imidazolium-Based Ionic Liquid with Molecular Liquids Depending on Their Electron-Donicity. *Phys. Chem. Chem. Phys.* **2014,** *16*, 23627-23638.
24. Shirota, H.; Kakinuma, S.; Itoyama, Y.; Umecky, T.; Takamuku, T. Effects of Tetrafluoroborate and Bis(Trifluoromethylsulfonyl)Amide Anions on the Microscopic Structures of 1-Methyl-3-Octylimidazolium-Based Ionic Liquids and Benzene Mixtures: A Multiple Approach by ATR-IR, NMR, and Femtosecond Raman-Induced Kerr Effect Spectroscopy. *J. Phys. Chem. B* **2016,** *120*, 513-526.
25. Hallett, J. P.; Welton, T. Room-Temperature Ionic Liquids: Solvents for Synthesis and Catalysis. 2. *Chem. Rev.* **2011,** *111*, 3508-3576.
26. Wang, H.; Gurau, G.; Rogers, R. D. Ionic Liquid Processing of Cellulose. *Chem. Soc. Rev.* **2012,** *41*, 1519-1537.
27. Shimizu, K.; Costa Gomes, M. F.; Pádua, A. A. H.; Rebelo, L. P. N.; Canongia Lopes, J. N. Three Commentaries on the Nano-Segregated Structure of Ionic Liquids. *J. Mol. Struct.: THEOCHEM* **2010,** *946*, 70-76.
28. Shimizu, K.; Bernardes, C. E. S.; Canongia Lopes, J. N. Structure and Aggregation in the 1-Alkyl-3-Methylimidazolium Bis(Trifluoromethylsulfonyl)Imide Ionic Liquid Homologous Series. *J. Phys. Chem. B* **2014,** *118*, 567-576.
29. Červinka, C.; Pádua, A. A. H.; Fulem, M. Thermodynamic Properties of Selected Homologous Series of Ionic Liquids Calculated Using Molecular Dynamics. *J. Phys. Chem. B* **2016,** *120*, 2362–2371.
30. Köddermann, T.; Reith, D.; Ludwig, R. Comparison of Force Fields on the Basis of Various Model Approaches—How to Design the Best Model for the $[C_nmim][NTf_2]$ Family of Ionic Liquids. *ChemPhysChem* **2013,** *14*, 3368-3374.
31. Marekha, B. A.; Koverga, V. A.; Moreau, M.; Kiselev, M.; Takamuku, T.; Kalugin, O. N.; Idrissi, A. Intermolecular Interactions, Ion Solvation, and Association in Mixtures of 1-*N*-Butyl-3-Methylimidazolium Hexafluorophosphate and Γ-Butyrolactone: Insights from Raman Spectroscopy. *J. Raman Spectrosc.* **2015,** *46*, 339-352.
32. Giernoth, R. NMR Spectroscopy in Ionic Liquds. In *Ionic Liquids*, Kirchner, B., Ed. Springer Berlin Heidelberg: 2010; Vol. 290, pp 263-283.

33. Damodaran, K. Recent NMR Studies of Ionic Liquids. In *Annual Reports on NMR Spectroscopy*, Academic Press: 2016; Vol. 88, pp 215–244.
34. Kiefer, J. Vibrational Spectroscopy for Studying Hydrogen Bonding in Imidazolium Ionic Liquids and Their Mixtures with Cosolvents. In *Hydrogen Bonding and Transfer in the Excited State*, John Wiley & Sons, Ltd: 2010; Vol. I & II, pp 341-352.
35. Ramya, K. R.; Kumar, P.; Venkatnathan, A. Molecular Simulations of Anion and Temperature Dependence on Structure and Dynamics of 1-Hexyl-3-Methylimidazolium Ionic Liquids. *J. Phys. Chem. B* **2015,** *119*, 14800-14806.
36. Zhang, S.; Shi, R.; Ma, X.; Lu, L.; He, Y.; Zhang, X.; Wang, Y.; Deng, Y. Intrinsic Electric Fields in Ionic Liquids Determined by Vibrational Stark Effect Spectroscopy and Molecular Dynamics Simulation. *Chem. – Eur. J.* **2012,** *18*, 11904-11908.
37. Stark, A.; Brehm, M.; Brüssel, M.; Lehmann, S. C.; Pensado, A.; Schöppke, M.; Kirchner, B. A Theoretical and Experimental Chemist's Joint View on Hydrogen Bonding in Ionic Liquids and Their Binary Mixtures. In *Electronic Effects in Organic Chemistry*, Kirchner, B., Ed. Springer Berlin Heidelberg: 2014; Vol. 351, pp 149-187.
38. Weber, H.; Kirchner, B. Complex Structural and Dynamical Interplay of Cyano-Based Ionic Liquids. *J. Phys. Chem. B* **2016,** *120*, 2471–2483.
39. Weber, H.; Hollóczki, O.; Pensado, A. S.; Kirchner, B. Side Chain Fluorination and Anion Effect on the Structure of 1-Butyl-3-Methylimidazolium Ionic Liquids. *J. Chem. Phys.* **2013,** *139*, 084502.
40. Wilson, G. J.; Hollenkamp, A. F.; Pandolfo, A. G. Resolving Ambiguous Naming for an Ionic Liquid Anion. *Chemistry International - Newsmagazine for IUPAC* **2007,** *29*, 16-18.
41. MacFarlane, D. R.; Tachikawa, N.; Forsyth, M.; Pringle, J. M.; Howlett, P. C.; Elliott, G. D.; Davis, J. H.; Watanabe, M.; Simon, P.; Angell, C. A. Energy Applications of Ionic Liquids. *Energy Environ. Sci.* **2014,** *7*, 232-250.
42. Skarmoutsos, I.; Welton, T.; Hunt, P. A. The Importance of Timescale for Hydrogen Bonding in Imidazolium Chloride Ionic Liquids. *Phys. Chem. Chem. Phys.* **2014,** *16*, 3675-3685.
43. Todorov, I. T.; Smith, W.; Trachenko, K.; Dove, M. T. DL_POLY_3: New Dimensions in Molecular Dynamics Simulations Via Massive Parallelism. *J. Mater. Chem.* **2006,** *16*, 1911-1918.
44. Martínez, L.; Andrade, R.; Birgin, E. G.; Martínez, J. M. Packmol: A Package for Building Initial Configurations for Molecular Dynamics Simulations. *J. Comput. Chem.* **2009,** *30*, 2157-2164.
45. Yong, C. W. DL_FIELD - a Force Field and Model Development Tool for DL_POLY. In *CSE Frontier, STFC Computational Science and Engineering*, Blake, R., Ed. Daresbury Laboratory, 2010; pp 38-40.
46. Canongia Lopes, J. N.; Deschamps, J.; Pádua, A. A. H. Modeling Ionic Liquids Using a Systematic All-Atom Force Field. *J. Phys. Chem. B* **2004,** *108*, 2038-2047.
47. Canongia Lopes, J. N.; Pádua, A. A. H. Molecular Force Field for Ionic Liquids Composed of Triflate or Bistriflylimide Anions. *J. Phys. Chem. B* **2004,** *108*, 16893-16898.
48. Canongia Lopes, J. N.; Pádua, A. A. H. Molecular Force Field for Ionic Liquids Iii: Imidazolium, Pyridinium, and Phosphonium Cations; Chloride, Bromide, and Dicyanamide Anions. *J. Phys. Chem. B* **2006,** *110*, 19586-19592.
49. Mondal, A.; Balasubramanian, S. A Molecular Dynamics Study of Collective Transport Properties of Imidazolium-Based Room-Temperature Ionic Liquids. *J. Chem. Eng. Data* **2014,** *59*, 3061-3068.
50. Andersen, H. C. Rattle: A "Velocity" Version of the Shake Algorithm for Molecular Dynamics Calculations. *J. Comput. Phys.* **1983,** *52*, 24-34.
51. Gabl, S.; Schröder, C.; Steinhauser, O. Computational Studies of Ionic Liquids: Size Does Matter and Time Too. *J. Chem. Phys.* **2012,** *137*, 094501.
52. Essmann, U.; Perera, L.; Berkowitz, M. L.; Darden, T.; Lee, H.; Pedersen, L. G. A Smooth Particle Mesh Ewald Method. *J. Chem. Phys.* **1995,** *103*, 8577-8593.
53. Melchionna, S.; Ciccotti, G.; Lee Holian, B. Hoover NPT Dynamics for Systems Varying in Shape and Size. *Mol. Phys.* **1993,** *78*, 533-544.
54. Hoover, W. G. Canonical Dynamics: Equilibrium Phase-Space Distributions. *Phys. Rev. A* **1985,** *31*, 1695-1697.

55. Brehm, M.; Kirchner, B. Travis - a Free Analyzer and Visualizer for Monte Carlo and Molecular Dynamics Trajectories. *J. Chem. Inf. Model.* **2011,** *51*, 2007-2023.
56. Bowron, D. T.; D'Agostino, C.; Gladden, L. F.; Hardacre, C.; Holbrey, J. D.; Lagunas, M. C.; McGregor, J.; Mantle, M. D.; Mullan, C. L.; Youngs, T. G. A. Structure and Dynamics of 1-Ethyl-3-Methylimidazolium Acetate Via Molecular Dynamics and Neutron Diffraction. *J. Phys. Chem. B* **2010,** *114*, 7760-7768.
57. Kohagen, M.; Brehm, M.; Thar, J.; Zhao, W.; Müller-Plathe, F.; Kirchner, B. Performance of Quantum Chemically Derived Charges and Persistence of Ion Cages in Ionic Liquids. A Molecular Dynamics Simulations Study of 1-*N*-Butyl-3-Methylimidazolium Bromide. *J. Phys. Chem. B* **2011,** *115*, 693-702.
58. Brehm, M.; Weber, H.; Pensado Alfonso, S.; Stark, A.; Kirchner, B. Liquid Structure and Cluster Formation in Ionic Liquid/Water Mixtures – an Extensive Ab Initio Molecular Dynamics Study on 1-Ethyl-3-Methylimidazolium Acetate/Water Mixtures – Part 2. *Z. Phys. Chem.* **2013,** *227*, 177-203.
59. Vyalov, I.; Kiselev, M.; Tassaing, T.; Soetens, J. C.; Idrissi, A. Investigation of the Local Structure in Sub and Supercritical Ammonia Using the Nearest Neighbor Approach: A Molecular Dynamics Analysis. *J. Phys. Chem. B* **2010,** *114*, 15003-15010.
60. Idrissi, A.; Gerard, M.; Damay, P.; Kiselev, M.; Puhovsky, Y.; Cinar, E.; Lagant, P.; Vergoten, G. The Effect of Urea on the Structure of Water: A Molecular Dynamics Simulation. *J. Phys. Chem. B* **2010,** *114*, 4731-4738.
61. Idrissi, A.; Vyalov, I.; Damay, P.; Frolov, A.; Oparin, R.; Kiselev, M. Assessment of the Spatial Distribution in Sub- and Supercritical CO_2 Using the Nearest Neighbor Approach: A Molecular Dynamics Analysis. *J. Phys. Chem. B* **2009,** *113*, 15820-15830.
62. Hardacre, C.; McMath, S. E. J.; Nieuwenhuyzen, M.; Bowron, D. T.; Soper, A. K. Liquid Structure of 1, 3-Dimethylimidazolium Salts. *J. Phys.: Condens. Matter* **2003,** *15*, S159–S166.
63. Hardacre, C.; Holbrey, J. D.; Mullan, C. L.; Youngs, T. G. A.; Bowron, D. T. Small Angle Neutron Scattering from 1-Alkyl-3-Methylimidazolium Hexafluorophosphate Ionic Liquids ($[C_n mim][PF_6]$, N=4, 6, and 8). *J. Chem. Phys.* **2010,** *133*, 074510.
64. Deetlefs, M.; Hardacre, C.; Nieuwenhuyzen, M.; Padua, A. A. H.; Sheppard, O.; Soper, A. K. Liquid Structure of the Ionic Liquid 1,3-Dimethylimidazolium Bis{(Trifluoromethyl)Sulfonyl}Amide. *J. Phys. Chem. B* **2006,** *110*, 12055-12061.
65. Hardacre, C.; Holbrey, J. D.; McMath, S. E. J.; Bowron, D. T.; Soper, A. K. Structure of Molten 1,3-Dimethylimidazolium Chloride Using Neutron Diffraction. *J. Chem. Phys.* **2003,** *118*, 273-278.
66. Hardacre, C.; Holbrey, J. D.; Nieuwenhuyzen, M.; Youngs, T. G. A. Structure and Solvation in Ionic Liquids. *Acc. Chem. Res.* **2007,** *40*, 1146-1155.
67. Brussel, M.; Brehm, M.; Pensado, A. S.; Malberg, F.; Ramzan, M.; Stark, A.; Kirchner, B. On the Ideality of Binary Mixtures of Ionic Liquids. *Phys. Chem. Chem. Phys.* **2012,** *14*, 13204-13215.
68. Matthews, R. P.; Welton, T.; Hunt, P. A. Hydrogen Bonding and π- π Interactions in Imidazolium-Chloride Ionic Liquid Clusters. *Phys. Chem. Chem. Phys.* **2015,** *17*, 14437-14453.
69. Fumino, K.; Peppel, T.; Geppert-Rybczynska, M.; Zaitsau, D. H.; Lehmann, J. K.; Verevkin, S. P.; Kockerling, M.; Ludwig, R. The Influence of Hydrogen Bonding on the Physical Properties of Ionic Liquids. *Phys. Chem. Chem. Phys.* **2011,** *13*, 14064-14075.
70. Roth, C.; Peppel, T.; Fumino, K.; Köckerling, M.; Ludwig, R. The Importance of Hydrogen Bonds for the Structure of Ionic Liquids: Single-Crystal X-Ray Diffraction and Transmission and Attenuated Total Reflection Spectroscopy in the Terahertz Region. *Angew. Chem., Int. Ed.* **2010,** *49*, 10221-10224.
71. Gilli, G.; Gilli, P. *The Nature of the Hydrogen Bond: Outline of a Comprehensive Hydrogen Bond Theory*. Oxford University Press: 2009; p 317.
72. Chang, H.-C.; Jiang, J.-C.; Chang, C.-Y.; Su, J.-C.; Hung, C.-H.; Liou, Y.-C.; Lin, S. H. Structural Organization in Aqueous Solutions of 1-Butyl-3-Methylimidazolium Halides: A High-Pressure Infrared Spectroscopic Study on Ionic Liquids. *J. Phys. Chem. B* **2008,** *112*, 4351-4356.
73. Cha, S.; Ao, M.; Sung, W.; Moon, B.; Ahlstrom, B.; Johansson, P.; Ouchi, Y.; Kim, D. Structures of Ionic Liquid-Water Mixtures Investigated by IR and NMR Spectroscopy. *Phys. Chem. Chem. Phys.* **2014,** *16*, 9591-9601.

74. Matthews, R. P.; Ashworth, C.; Tom, W.; Patricia, A. H. The Impact of Anion Electronic Structure: Similarities and Differences in Imidazolium Based Ionic Liquids. *J. Phys.: Condens. Matter* **2014,** *26*, 284112.
75. Khrizman, A.; Cheng, H. Y.; Bottini, G.; Moyna, G. Observation of Aliphatic C-H···X Hydrogen Bonds in Imidazolium Ionic Liquids. *Chem. Commun*. **2015,** *51*, 3193-3195.
76. Marekha, B. A.; Kalugin, O. N.; Bria, M.; Buchner, R.; Idrissi, A. Translational Diffusion in Mixtures of Imidazolium ILs with Polar Aprotic Molecular Solvents. *J. Phys. Chem. B* **2014,** *118*, 5509–5517.
77. Russina, O.; Triolo, A. New Experimental Evidence Supporting the Mesoscopic Segregation Model in Room Temperature Ionic Liquids. *Faraday Discuss.* **2012,** *154*, 97-109.
78. Russina, O.; Triolo, A.; Gontrani, L.; Caminiti, R. Mesoscopic Structural Heterogeneities in Room-Temperature Ionic Liquids. *J. Phys. Chem. Lett.* **2011,** *3*, 27-33.
79. Avent, A. G.; Chaloner, P. A.; Day, M. P.; Seddon, K. R.; Welton, T. Evidence for Hydrogen Bonding in Solutions of 1-Ethyl-3-Methylimidazolium Halides, and Its Implications for Room-Temperature Halogenoaluminate(III) Ionic Liquids. *J. Chem. Soc., Dalton Trans.* **1994**, 3405-3413.
80. Bonhôte, P.; Dias, A.-P.; Papageorgiou, N.; Kalyanasundaram, K.; Grätzel, M. Hydrophobic, Highly Conductive Ambient-Temperature Molten Salts. *Inorg. Chem.* **1996,** *35*, 1168-1178.
81. Mele, A.; Tran, C. D.; De Paoli Lacerda, S. H. The Structure of a Room-Temperature Ionic Liquid with and without Trace Amounts of Water: The Role of C-H···O and C-H···F Interactions in 1-N-Butyl-3-Methylimidazolium Tetrafluoroborate. *Angew. Chem., Int. Ed.* **2003,** *42*, 4364-4366.
82. Choudhury, A. R.; Winterton, N.; Steiner, A.; Cooper, A. I.; Johnson, K. A. In Situ Crystallization of Low-Melting Ionic Liquids. *J. Am. Chem. Soc.* **2005,** *127*, 16792-16793.
83. Hamaguchi, H.-O.; Ozawa, R. Structure of Ionic Liquids and Ionic Liquid Compounds: Are Ionic Liquids Genuine Liquids in the Conventional Sense? In *Advances in Chemical Physics*, John Wiley & Sons, Inc.: 2005; Vol. 131, pp 85-104.
84. Izgorodina, E. I.; Rigby, J.; MacFarlane, D. R. Large-Scale *Ab Initio* Calculations of Archetypical Ionic Liquids. *Chem. Commun.* **2012,** *48*, 1493-1495.
85. Cabaço, M. I.; Besnard, M.; Danten, Y.; Coutinho, J. A. P. Solubility of CO_2 in 1-Butyl-3-Methyl-Imidazolium-Trifluoro Acetate Ionic Liquid Studied by Raman Spectroscopy and DFT Investigations. *J. Phys. Chem. B* **2011,** *115*, 3538-3550.
86. Danten, Y.; Cabaço, M. I.; Besnard, M. Interaction of Water Diluted in 1-Butyl-3-Methyl Imidazolium Ionic Liquids by Vibrational Spectroscopy Modeling. *J. Mol. Liq.* **2010,** *153*, 57-66.
87. Pensado, A. S.; Brehm, M.; Thar, J.; Seitsonen, A. P.; Kirchner, B. Effect of Dispersion on the Structure and Dynamics of the Ionic Liquid 1-Ethyl-3-Methylimidazolium Thiocyanate. *ChemPhysChem* **2012,** *13*, 1845-1853.
88. Wendler, K.; Zahn, S.; Dommert, F.; Berger, R.; Holm, C.; Kirchner, B.; Delle Site, L. Locality and Fluctuations: Trends in Imidazolium-Based Ionic Liquids and Beyond. *J. Chem. Theory Comput.* **2011,** *7*, 3040-3044.

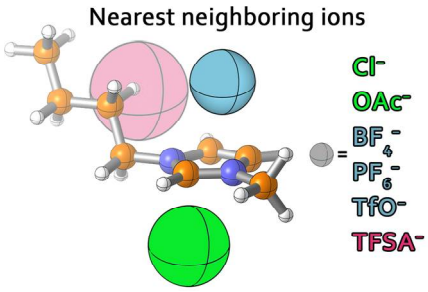
Nearest neighboring ions
Cl-
OAc-
BF4-
PF6-
TfO-
TFSA-